JOURNAL OF THERMOPHYSICS AND HEAT TRANSFER
Vol. 7, No. 3, July–Sept. 1993

Thermal Analysis and Test of Laser Reference Cavity

R. M. Amundsen*
NASA Langley Research Center, Hampton, Virginia 23681

SUNLITE is a space-based experiment which uses an external reference cavity to provide a stable frequency reference for a terahertz laser oscillator. Thermal stability of the cavity is a key factor in attaining a stable narrow-linewidth laser beam. This article describes the thermal stability requirements on the cavity design and detailed thermal analysis performed, as well as thermal testing that was performed on a prototype. Analytical thermal models were correlated to the test data. Cavity design was improved based on lessons learned in the prototype; additional modeling of the current design is presented. Suggestions for improving similar high-precision thermal tests are given.

Introduction

THE SUNLITE (originally Stanford University—NASA Laser In-Space Technology Experiment) instrument is being developed by NASA Langley Research Center to validate the fundamental linewidth and frequency stability limits of a neodymium yttrium aluminum garnet (Nd:YAG) laser oscillator, locked to a high-finesse reference cavity, in the microgravity and vibration-free environment of space. Heterodyne beat linewidths of diode-pumped solid-state laser oscillators of 0.33 Hz have been achieved in the laboratory.[1-3] Efforts to stabilize lasers in Earth-based laboratories have been limited by sensitivity of the apparatus to vibrational noise and distortions in the reference cavity induced by gravity.[4] A free-flying experiment in the microgravity and vibration-free environment of space would greatly reduce these limitations. The SUNLITE program will provide an automated and self-contained stabilized terahertz oscillator, and will characterize the operation of this oscillator system in space. The low vibrational noise in the space environment will aid in bringing the linewidth closer to the shot noise limit of the system. Among the many applications of such an ultrastable laser in space are deep space coherent communications, astrometry, laser radar for location and docking, and laser-gyro rotation sensors. Ultranarrow linewidth lasers will also enable investigations such as the detection of gravity waves and tests of the theory of relativity.[5]

The lasers on the SUNLITE instrument are externally stabilized by a frequency-modulation technique. This technique uses a Fabry-Perot reference cavity with ultrahigh reflectance mirrors to provide a stable cavity resonance frequency. A servo-loop feedback method is used to lock the laser frequency to the resonance frequency. The resonance frequency is determined by the cavity length; therefore, the frequency and heterodyne beat linewidth of the laser are extremely sensitive to changes in the length of the cavity. Performing this experiment in space avoids gravitational and vibrational distortions in the cavity. Once in space, the dominant effect on the cavity length will be thermal changes. These are due to fluctuations in the spacecraft temperature during an orbit, and also to optical bench heating produced by power dissipation of SUNLITE components. The cavity assembly is mounted on an optical bench which also carries the lasers and associated opto-electronic devices. The optical bench housing is completely enclosed within a free-flying spacecraft. In flight, the operation of the instrument will encompass 1 h, which includes three 10-min data-taking periods. During this time, all sources of mechanical noise will be quiescent.

The cavity is fabricated from a material with a low coefficient of thermal expansion to minimize the thermal effects, but the requirement on the temperature change of the cavity is still a demanding one. A practical limit that can be verified by direct thermal measurement is established by requiring that the thermal effect on frequency drift per minute not exceed the cavity linewidth. For the inherent 150-kHz linewidth of this cavity, this limits the length growth to less than 0.025 nm/min: a maximum thermal transient of 0.025°C/min. (Using $(dL/L) = (d\nu/\nu)$ and $dL = \alpha L \Delta T$, with $\alpha = 2 \times 10^{-8}$ m/m°C, $L = 50$ mm, $\nu = 3 \times 10^{14}$ Hz.) This limit is close to the resolution of the thermal measurement system that will be used to verify that this requirement has been met. However, the design goal is to produce performance much more stable than this requirement, and the predictions from analysis indicate that this can be accomplished.

In the laboratory environment, this level of thermal stability is often achieved by using either a series of thermal shields around the cavity to buffer the reaction to external changes, or thread-like isolating supports to minimize input from the external environment. For the SUNLITE experiment, the limitations on mass and volume for a space-flight experiment severely limit how much thermal buffering mass can be used in the cavity design. The requirement to survive launch vibrations entails modification of the isolation method. The design must provide adequate structural support to maintain the position and alignment of the cavity during testing and launch. The design of the passive cavity assembly has been accomplished using an isolation technique to limit the heat transfer between the optical bench and the cavity, while maintaining a low mass and stable alignment. A thermal balance test was performed to evaluate the performance of a prototype cavity mount design. This article will describe that thermal vacuum test, outline some improvements suggested for similar thermal tests, and describe thermal analysis performed on the current cavity assembly design.

Prototype Cavity Assembly Design

The original cavity assembly design incorporates several features to improve thermal isolation. As shown in Fig. 1, the inner spacer is a cylinder of low expansion glass with mirrors at each end. The "spider" which supports this is fabricated of Kel-F®, a thermoplastic with low thermal conduc-

Presented as Paper 92-0817 at the AIAA 30th Aerospace Sciences Meeting and Exhibit, Reno, NV, Jan. 6–9, 1992; received March 30, 1992; revision received July 27, 1992; accepted for publication July 28, 1992. Copyright © 1992 by the American Institute of Aeronautics and Astronautics, Inc. No copyright is asserted in the United States under Title 17, U.S. Code. The U.S. Government has a royalty-free license to exercise all rights under the copyright claimed herein for Governmental purposes. All other rights are reserved by the copyright owner.

*Aerospace Engineer, Systems Engineering Division, Thermal Analysis Section.

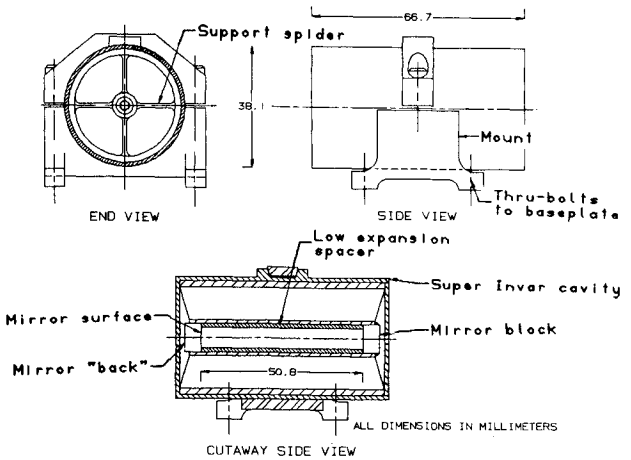

Fig. 1 Preliminary cavity assembly design.

tivity. The cylindrical case into which the spider slips is made of Super Invar®, a low thermal expansion iron-nickel alloy. The mounting feet, mount, and yoke which attach the case to the optical bench are also fabricated from Kel-F. The mounting feet have a small area of contact with the optical bench and a small effective conductance area to the main portion of the mount. Mirrors were not incorporated in the prototype since they 1) would not be used in the thermal test, 2) have negligible thermal effect, and 3) are extremely expensive. The inner spacer was manufactured from fused silica rather than low expansion glass in order to get similar thermal characteristics at lower cost. The low expansion qualities were not necessary for this prototype since there was no optical performance test. For the final cavity design, high-reflectance mirrors will be attached at the ends of the spacer and the cavity will have a finesse of over 20,000. Finesse is a figure of merit used to describe cavities; it is approximately equal to the number of times a light beam will bounce between the mirrors before being scattered, absorbed, or transmitted. Measurements on recently fabricated cavities have established that their average finesse is 150,000, measured both by photon lifetime and by a free spectral range method.

The glass to be used for the flight spacer was selected for low coefficient of thermal expansion (CTE); the grade selected at this stage of the design had a vendor-specified CTE value of 2×10^{-8} m/m°C over the range 5–35°C. The thermal changes in length between the mirrors will be determined by the sum of the material which connects the mirrors. The mirror blocks themselves do not contribute to the change in length, since the mirrored surfaces are on the faces connected to the spacer. The preferred method for joining the mirrors to the spacer is an optical bond: a bond directly between the glass surfaces which would not add to the overall CTE. The thermal requirements presented here assume that an overall cavity CTE value of 2×10^{-8} m/m°C is achievable.

The development of the reference cavity assembly is an iterative process and several designs will be analyzed, built, and tested. The thermal isolation of this prototype design was not optimum; it was improved in a subsequent design, as discussed later.

Test Objectives

The thermal stability is essential to the successful operation of the instrument, and the requirement is severe enough to challenge the limits of analytical predictions. Testing of the prototype design provides confidence in the design technique, and yields data that can be used to correlate the analytical model. The objectives of this primary test are to verify that the isolation technique will sufficiently limit the thermal transient and gather data to correlate the analytical thermal model. In flight, the cavity must remain stable for 1 h after the start of operation. This test was not a flight simulation; thermal

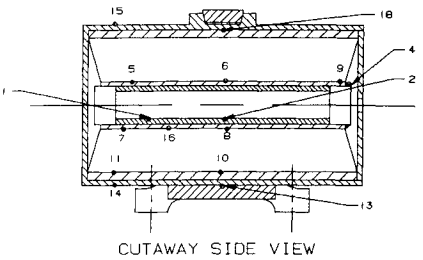

Fig. 2 Temperature sensor placement.

profiles of the baseplate for each day encompassed a wide range of rates and ranges. Future tests will incorporate a functioning cavity and laser to evaluate the effect of laser beam heating and ensure accuracy of the analytical model.

Test Setup

The SUNLITE thermal vacuum test consisted of four test days, with a different thermal cycle performed each day. The thermal response of the prototype cavity assembly was measured by 15 temperature sensors (Omega AD590). The sensors were placed on the reference cavity assembly as shown in Fig. 2. The sensor no. 1 reading is referenced most often since it represents the spacer temperature, which is critical in determining thermal growth between the mirrors. Two sensors were used to monitor the temperature of the baseplate. The cavity mount was bolted to the baseplate, which simulated changes in temperature of the optical bench. The test was conducted in a vacuum to eliminate gas conduction and convective effects. The cavity assembly was blanketed with multilayer insulation (MLI) to minimize radiative thermal effects and more closely simulate a flight environment. The temperature of the baseplate was computer-controlled to match the desired profile. The control system used four infrared heat lamps directed at one side of the baseplate, and computer-controlled LN_2 flow through coils attached to the baseplate.

The AD590 temperature sensors are current output devices which deliver a current proportional to their temperature. These currents were transformed to proportional voltages through a transconductance amplifier. The voltages were read and corresponding temperatures calculated by a Fluke datalogger. An automated program saved all test temperatures to three decimal places at 2-min intervals.

Data Evaluation

The temperature sensors have a maximum absolute error rating of 2°C, and a maximum repeatability error of 0.1°C/month. The potential absolute errors are not cause for concern since what is being measured is a change over time of each sensor reading; the error from an absolute temperature is not crucial. To minimize the absolute errors between the sensor readings, each cycle was initiated with a steady state. The test setup was allowed to equilibrate in a passive mode overnight, so that at the test start all sensors would be stable and at or near the same temperature. The calculated reference temperature was an average of all sensor readings at the initial time. This temperature was subtracted from each sensor's initial reading to give a correction factor used for that sensor on that test day. The use of an average temperature as the reference to correct the sensor readings did incorporate slight errors, since the sensors were not at precisely the same initial temperature, but these were less than the potential 2°C absolute error. This correction does not affect the crucial parameters of stability and resolution for each sensor.

The values that are generated here for the cavity thermal stability should be overestimates of the rate of change for several reasons. First, the sensors used had an internal heat dissipation of 1.5 mW. This power is responsible for a small portion of the sensor-indicated rise in temperature, especially for day 2, when the sensors were powered up not long before

Table 1 Initial test conditions

Test day	Stability, °C/min	Start temperature, °C	Baseplate ramp, °C/h
1	0.00075	24.815	+30
2	0.0075	23.842	+60
3	−0.0028	23.109	−15
4	−0.006	22.924	+3.6

the start of the test. In the analytical model, this power dissipation is accounted for by heat sources at each sensor. Another factor is the thermal impact of the wires that connect the sensors to the ambient environment. Long sections of 30-gauge wire were used to minimize thermal input and impact on the thermal rate of change. These wires, being connected to the external environment, add a thermal path that does not exist in the flight configuration; thus they should add a conservative factor to the values for temperature change measured here.

Table 1 shows the initial stability of sensor no. 1, the averaged reference temperature, and the baseplate ramp rate for each day of testing. The stability is calculated from the drift in the last 5 min before the start of the test. The drift rates for each day were added to, or subtracted from, the measured temperature rise to give worst-case rate values. The relatively high values for drift rate are due to the drift of the entire building and facility overnight. This can be corrected in future tests, as described in the conclusions section.

This data analysis method of taking the worst of all cases may seem overconservative, but in fact there are mitigating factors. The sensors are each mounted on a small slab of room temperature vulcanization (RTV) adhesive, so that there is some thermal isolation between the sensor and the associated structure. Therefore, there is a slight time lag between the increase of the cavity temperature and the increase in the sensor temperature; in other words, the actual temperature rise could be faster than the recorded temperature rise. The variation in the thickness of these pads of adhesive leads to relative errors between sensors. The reference correction performed to eliminate the variability error between sensors can introduce small relative errors due to initial differences in temperature. This potential error, and that due to the variation in adhesive bonds, make the relative values between the sensors less reliable than the change in one sensor reading with time. For this reason, the analytical model will be correlated using the changes in each sensor with time, and not differences between sensor readings.

Test Results

The test profiles for each of the four days are shown in Figs. 3–6. The baseplate temperature and the reading of sensor no. 1 on the spacer are plotted. It can be determined from these graphs that the ramp rate observed at the cavity is reduced by a factor of approximately 20, and the steady-state plateau of the cavity is far removed from the baseplate plateau. This is an indication of the thermal isolation of the cavity.

The thermal ramp for day 1 (30°C/h) is much more severe than any potential flight ramp. The data can be interpolated to reflect flight-like results using the rough guideline that the ramp rate will have a linear effect on the cavity transient. A ramp value for worst-case flight conditions derived from preliminary optical bench modeling is 6°C/h. This exact value was not used as a test ramp because modeling was not complete when the ramps were selected. The measured transient from the first hour is multiplied by the ratio of 6°C/h and the test ramp rate to find the predicted flight transient. This approximation factor cannot be used in lieu of detailed modeling, but it gives an estimate of the temperature rise for flight-like conditions. This interpolation technique is supported by the analytical model. Later optical bench modeling has indicated that the worst-case flight conditions will not be as severe as 6°C/h; a maximum of 2°C/h is anticipated. Thus, the interpolated results presented here are conservative.

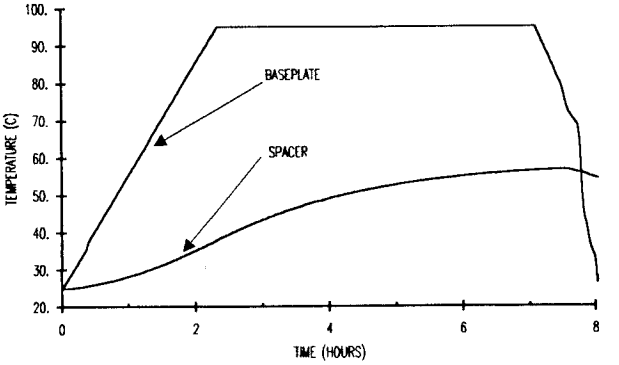

Fig. 3 Temperature profiles for test day 1.

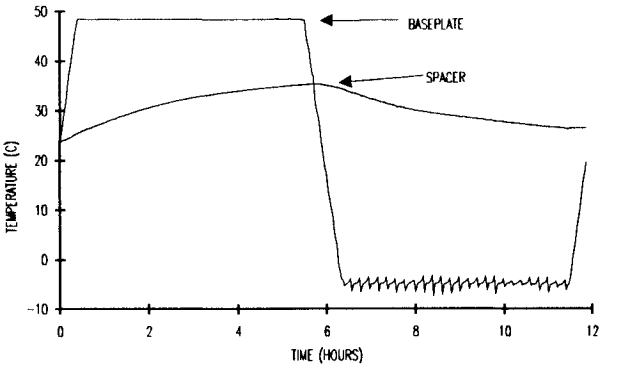

Fig. 4 Temperature profiles for test day 2.

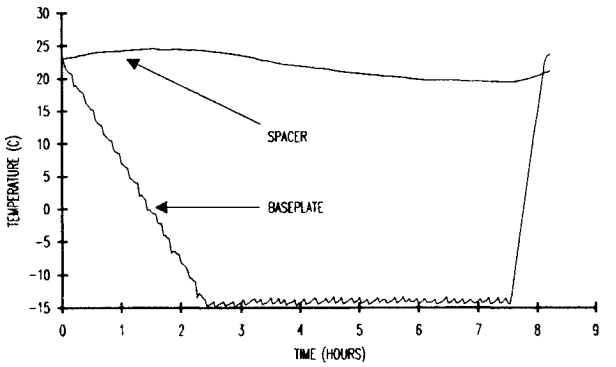

Fig. 5 Temperature profiles for test day 3.

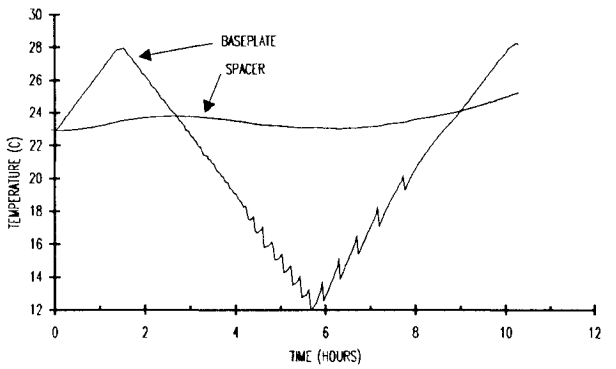

Fig. 6 Temperature profiles for test day 4.

Table 2 shows the interpolated results for each test day; this design easily meets the imposed limit on the thermal rate, even with worst-case conditions on the optical bench. The values for day 2 are lower since the heating ramp levels off before 1 h.

Table 2 Interpolated rates for 6°C/h ramp

Test day	Maximum rate at 1 h, °C/min	Average rate over 1 h, °C/min
1	0.017	0.011
2	0.009	0.006
4	0.014	0.013

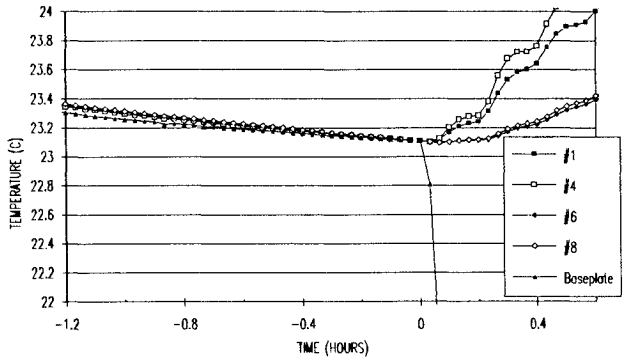

Fig. 7 Pretest temperatures for day 3.

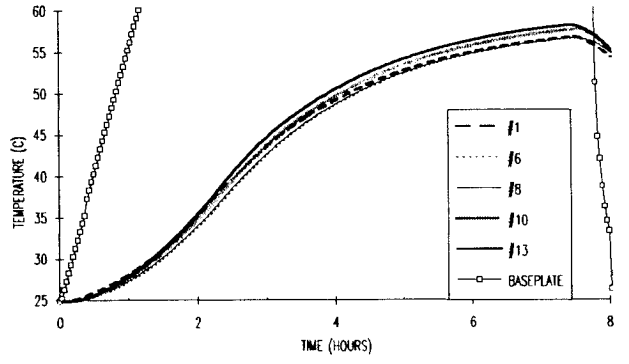

Fig. 8 Selected sensors for day 1.

The pretest stability curves for each of the test days showed normal behavior; the only exception was day 3. Several pretest sensor values are shown in Fig. 7; all the sensors are going through a similar slight temperature decrease before the downward ramp begins, at which point they all deviate upward. This was the only test to initiate with a downward ramp; when the LN_2 lines begin full flow to initiate cooling, and the IR lamps are activated to vaporize the liquid in the lines, there could be some anomalous radiative heating effect into the cavity assembly. Another possible cause would be that the warping of the baseplate was most severe at the start of this test due to the combined effects of lamps and LN_2. This could cause the mounting feet to lose contact with the baseplate and reduce conduction so that the self-heating of the sensors dominated.

Thermal responses of sensors encompassing the main positions on the cavity assembly for day 1 are shown in Fig. 8. The main point to be elicited from these curves is that the significant isolation is evidently being accomplished between the baseplate and the foot of the cavity mount, since the sensors are all showing a similar large temperature delta from the baseplate. The small conductive area of the Kel-F feet is effective in reducing the heat flow into the cavity mount.

Test Conclusions and Concerns

Cavity Assembly Performance

The cavity thermal isolation performance was better than the requirement of 0.025°C/min in all cases. This was true even when unrealistically worst-case conditions were assumed. The mount is damping the initial effect of baseplate temperature change rates by at least a factor of 20. The main isolation is being accomplished in the Kel-F mounting feet and mount; the thermal isolating effect of the spider is outweighed by the effect of the small thermal conductance through the mounting feet.

Test System

The test system thermal stability before testing each day was not as good as could be expected, as seen in Table 1. Part of this was due to drift of the building itself, and some was induced by evacuation of the system and power-up. In general, for any future tests, the baseplate will be kept under active thermal control during the entire testing period, as well as being actively stabilized in an evacuated, power-on condition for at least 12 h before the start of the first test. One reason this was not done was because of the "noise" inherent in any thermal control system; it was felt that a passively stable baseplate temperature was more valuable than a continuously controlled, slightly oscillating baseplate temperature. For this experiment, because of the isolation of the critical part (i.e., the cavity), the slight thermal oscillation of an actively controlled baseplate would probably be more acceptable than long-term drift.

The liquid nitrogen system used an "on-off" control, which produced large swings in the baseplate temperature at the lower temperatures, as can be seen in the baseplate temperature profiles in Figs. 4–6. The LN_2 line performance has been improved since this test. Liquid nitrogen flow is now controlled by a digital valve system which allows a resolution on flow control of one part in eight. This produces a much smoother temperature decrease ramp, and more stable soaks at low temperatures. Some other options which could assist in correlation of the model and transfer of the information to a flight configuration are 1) to use a baseplate ramp which is as close as possible to the nominal flight ramp, and ramps slightly more and less severe; 2) to run ramps which are symmetrical in increasing and decreasing temperature to ensure that there is no thermal directional bias in the test set-up; 3) to ramp only the radiative environment in order to directly evaluate this effect; 4) to run a steady-state case with differing baseplate and radiative temperatures; and 5) to use MLI which is as close as possible to the flight configuration.

Sensor Selection and Attachment

The current output aspect of the monolithic integrated circuit sensors is advantageous for vacuum test use, since they can be attached with little regard for the temperatures and materials at each electrical joint. The correction of all sensor readings based on an initial average temperature affects only the absolute reading of each sensor; the relative reading of each sensor (i.e., the change in the reading of one sensor over time) is still highly accurate. From the vendor-specified stability over one month, it can be seen that the stability over an 8-h test day is at the 0.001°C level. The extrapolations to flight conditions and correlation of the analytical model were made using the changes in single sensor values.

The main concern with these sensors for this type of test is that they dissipate 1.5 mW per sensor for a total of 22.5 mW within the cavity assembly. From the analytical model, heating on the order of tens of microwatts can be seen to change the cavity heating rate significantly. Differing amounts of RTV adhesive under each sensor, as well as the different substrates, produced dissimilar thermal environments at each sensor. The self-heating of the sensors can be included in the analytical model, but without a detailed analysis of the thermal environment of each sensor, the determination of the actual temperature at each sensor location over time is an almost impossible task. In general, when temperatures are to be measured to this accuracy, it would be recommended to use passive sensors that dissipate little or no power.

The sensor proposed for future tests is a newly available miniature thermistor which claims a calibration of 0.01°C

traceable to National Institute for Standards and Technology (NIST). These thermistors have a room temperature resistance of about 10 kΩ, and exceptionally steep resistance vs temperature properties. With suitable measurement techniques, i.e., low measurement voltage, the dissipated power can be kept below 0.1 mW per sensor. As few as possible of these sensors should be within the cavity assembly, since power dissipated within the assembly will have the most impact on the cavity temperature. The optimum method for attaching the sensors would be a thermally conductive epoxy, such as one that is metal filled. Metallic tape or a metal mesh pad within the adhesive are also possibilities. More rigorous controls on the thickness of the bonding pad below the sensor would aid in equalizing the thermal resistance environment of each sensor. The suggested epoxy for future tests is a thin-film conductive adhesive used for electronic hybrids which has a uniform film thickness of 0.13 mm.

Analytical Thermal Model Correlation

An analytical thermal model of the cavity assembly was constructed to allow correlation with the test results, as well as thermal predictions for the flight system. The model was originally built as a solid geometry model in PATRAN® and was translated to the thermal analysis software systems integrated numerical differencing analyzer—1985 version (SINDA-85). Figure 9 shows the solid geometry model and the nodal divisions used. An advantage of using PATRAN in this type of application is the ability to produce color thermal maps of the results, which help in gaining an overall understanding of the driving mechanisms, and also aid in debugging the model. The nodes and linear conductors were calculated by the PATSIN translator; this uses the geometry and materials from the PATRAN model to create nodes and linear conductors in a SINDA model. SINDA uses a lumped-mass representation of the system and solves for transient and steady-state temperatures using a finite difference method. The radiation conductors were calculated using the TRASYS software; the TRASYS model geometry was identical to the PATRAN model. The radiative conductors created were used in the analytical thermal model. Additional nodes and conductors were added for the test baseplate, thermal sensors, and MLI. The model consisted of 428 thermal nodes, 966 linear conductors, and 1502 radiation conductors.

The model was run with boundary conditions on the baseplate simulating each of the four test days. The full power of 1.5 mW was applied to each sensor node, since this was found to give the best correlations. Many parameters in the model were altered in the attempt to achieve the best possible correlation to all four days of data. The most critical items were found to be the attachment of the Kel-F mounting feet to the baseplate, and the radiation between the base of the mount and the baseplate. Parametric studies of the mounting feet conductors were carried out in SINDA. The radiation between the mount base and plate was more severe than it would have been for a flight configuration, since no MLI was placed

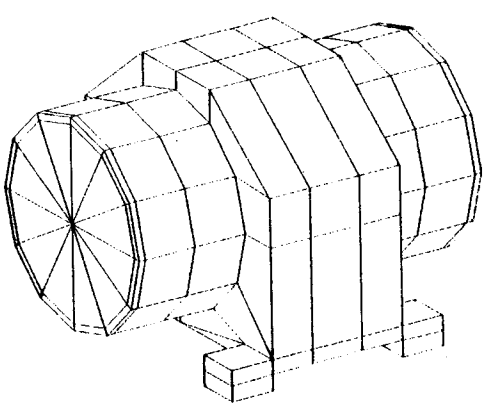

Fig. 9 PATRAN solid geometry model.

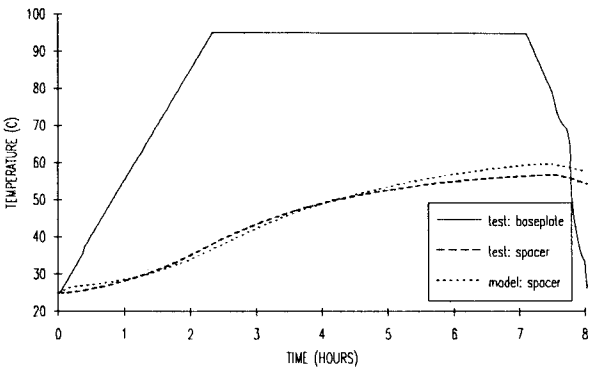

Fig. 10 Actual vs predicted—test day 1.

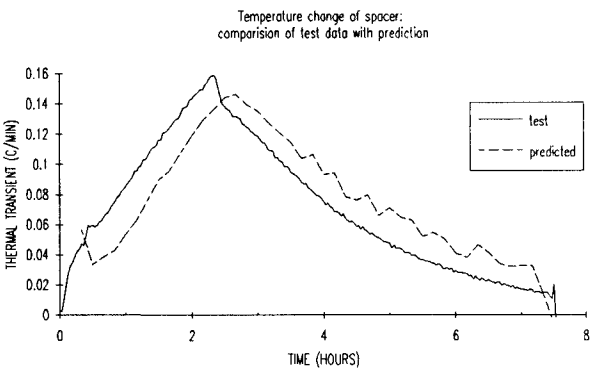

Fig. 11 Actual vs predicted—test day 1.

on the base of the mount for this test. For the flight model this value will not be a concern since that radiation will be reduced by MLI.

The cavity temperature predictions of the correlated model vs actual data for the first test day can be seen in Fig. 10. The fit of the prediction to the test data is seen to be fairly good. For this application, a better measure of the correlation is the transient experienced by the cavity. Figure 11 shows the correlation for the cavity transient; this transient is what will drive the rate of length change between the mirrors and, thus, the rate of frequency drift. The prediction of the maximum transient is within 9%, although it is displaced in time by about 20 min. Use of the transient is in fact a very sensitive and revealing way to measure model correlation, and one that highlights the most important prediction of the model. This method will be used for model correlation in future tests.

The cavity predictions for the remaining test days also follow the general shape of the test data fairly well, and are nearly always within 1°C or within 10% of the transient value. The correlation was not taken further since the cavity mount had already undergone significant re-design.

Cavity Assembly Redesign

The cavity assembly has undergone substantial redesign since the prototype was fabricated, due to structural, thermal, and optical requirements. A sketch of the new design is shown in Fig. 12; the housing end caps are removed so that the interior is visible. One major design change was the mounting scheme. The original design was based on using shims under the feet as required to attain alignment when mounting the cavity on the optical bench. Subsequent to that design, new alignment requirements were developed. Based on optical analysis, the following alignment tolerance requirements were generated: 25 μm in the two translational axes perpendicular to the optical axis, and 100 μrad in the two angular motions of pitch and yaw. Shimming does not have sufficient flexibility to allow successful alignment using the desired alignment method. A new mounting system was devised which uses fine thread screw feet at three mounting points to attain the re-

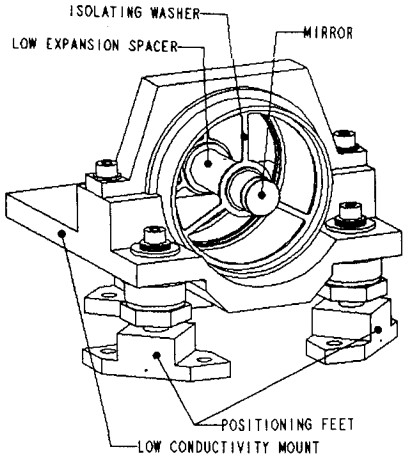

Fig. 12 Current cavity assembly design.

quired alignment resolution. The mating parts of these feet are fabricated from stainless steel and titanium.

The Kel-F used for the prototype mount had a CTE which is significantly higher than the other components on the optical bench, so the cavity would experience a greater height change due to a thermal shift. The difference could be on the order of 10 μm, which could cause unacceptable errors in the alignment. It is important that the mount be a low thermal conductivity material, since it is accomplishing much of the thermal isolation of the cavity. The material chosen is Ultem® 2300, a polyetherimide thermoplastic reinforced with 30% glass fibers. Ultem has better mechanical properties for this purpose than Kel-F, a CTE very close to that of aluminum, and thermal conductivity similar to Kel-F.

There were several concerns with the Kel-F spider within the sealed housing, including high outgassing, high CTE, the potential for cold flow, and difficulties in bonding. This led to replacing the Kel-F spider with a thin titanium alloy washer with substantial cutouts to reduce the thermal path. The glass used for the spacers and mirrors has been selected to be ULE® Corning 7971. A CTE lower than 2×10^{-8} m/m°C may be achievable; preliminary testing has given a value of 2×10^{-10} m/m°C.

Analytical Predictions for Current Design

The cavity assembly has been modeled in PATRAN. The node geometry is shown as a cutaway view in Fig. 13. These nodes are translated to SINDA; the mounting feet, optical bench structure, and power dissipations are added in the SINDA model.

The effect of the lasers in heating the mirrors by absorption is included in the thermal model. The original modeled finesse was 20,000 and the absorption was assumed to be 1 ppm, resulting in an absorbed power at each mirror of 85 μW. This modeling is being reworked for the actual measured parameters of the flight cavities. There are two laser beams incident on the cavity during the first experiment when two lasers are locked to one cavity, and one beam during the second experiment when each laser locks to a separate cavity. The second experiment uses two data-taking periods. A photoelectric detector which dissipates 1 mW is fastened to one end of the case.

The boundary conditions which drive the thermal drift of the cavity are the temperature changes on the optical bench where the cavity assembly is mounted. Starting from a stable condition, the power dissipations on the optical bench were input to produce the predicted variation in temperature of the optical bench and cavity. The predictions for the cavity temperatures and the transients over the operational hour are shown in Fig. 14. The relatively large initial transient is caused by the absorption of laser power at the mirrors. The maximum

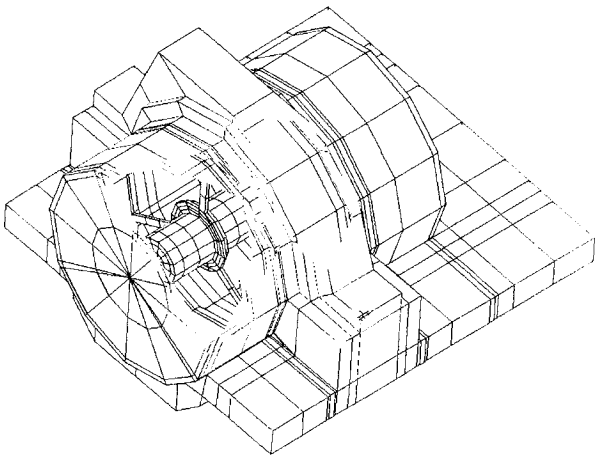

Fig. 13 Current design—PATRAN model.

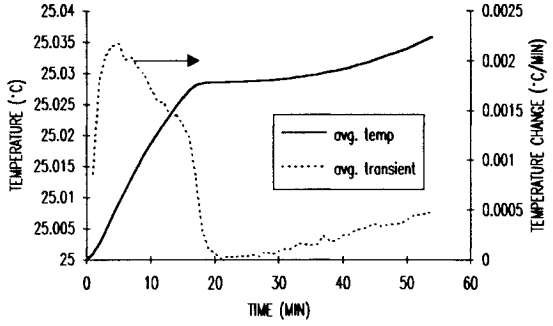

Fig. 14 Predicted cavity temperature and rate for stable start case.

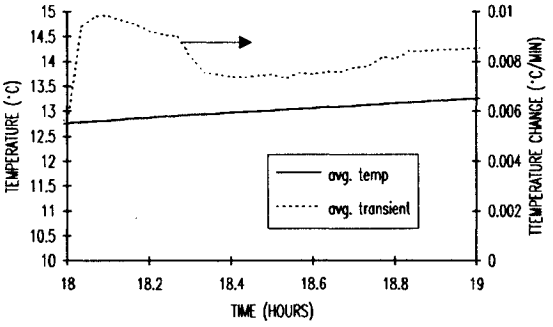

Fig. 15 Predicted cavity temperature and rate for spacecraft transient case.

transient on the cavity is 0.002°C/min, a factor of 10 below the maximum allowable of 0.025°C/min.

Another consideration is the long term effect of the change in spacecraft temperature on the cavity transient. A model of the entire instrument was analyzed which considered a change in temperature of the spacecraft only, and determined the time required for the maximum transient to reach the cavity. The time was found to be approximately 18 h after the onset of the maximum transient of the spacecraft. A prediction was made with startup at this 18-h time, thus beginning operation with the maximum transient on the cavity. The cavity temperature and transient for this case are shown in Fig. 15. The transient is more uniform and higher, with a maximum of 0.01°C/min, but is still well within the requirement.

Summary and Notes for Future Work

A thermally resistant design of a laser oscillator reference cavity assembly was developed to satisfy the demanding thermal stability requirements of the SUNLITE experiment. A prototype of this cavity assembly was fabricated and tested, achieving better than the thermal stability requirement of 0.025°C/min. An analytical model was developed using PATRAN, SINDA, and thermal radiation analysis system

(TRASYS) software, and was correlated to within 9% of thermal transient test data from the prototype.

The cavity assembly has undergone substantial redesign due to thermal and alignment requirements. The maximum predicted transient for the new design is about 0.01°C/min, which is well below the stability requirement. Due to the importance of the thermal performance and the high of resolution required of the thermal predictions, this new design has been fabricated and will be tested. Future tests will use the described strategies to improve the reliability and efficiency of the test system. This design has proven to be a thermally stable one which also incorporates novel features in terms of adjustability and materials.

Acknowledgments

The support and accomplishments of the entire SUNLITE team in the cavity conception, detailed design, and thermal test are gratefully acknowledged. Specific thanks are due to Alfred VonTheumer for work on the initial cavity assembly detailed design, Stephen Hughes for developing the current design, Charles Jenkins for support of the thermal testing, and Steve Sandford and Martin Buoncristiani for assistance in technical editing and content.

References

[1]Day, T., Nilsson, A. C., Fejer, M. M., Farinas, A. D., Gustafson, E. K., Nabors, C. D., and Byer, R. L., "30 Hz-Linewidth, Diode-Laser-Pumped, Nd:GGG Nonplanar Ring Oscillators by Active Frequency Stabilization," *Electronics Letters*, Vol. 25, No. 13, 1989, pp. 810, 811.

[2]Day, T., Gustafson, E. K., and Byer, R. L., "Active Frequency Stabilization of a 1.062-mm, Nd:GGG, Diode-Laser-Pumped Nonplanar Ring Oscillator to Less than 3 Hz of Relative Linewidth," *Optics Letters*, Vol. 15, No. 4, 1990, pp. 221–223.

[3]Day, T., "Frequency Stabilized Solid State Lasers for Coherent Optical Communications," Ph.D. Dissertation, Stanford Univ., Stanford, CA, Sept. 1990.

[4]Salomon, C., Hils, D., and Hall, J. D., "Laser Stabilization at the Millihertz Level," *Journal of the Optical Society of America B*, Vol. 5, No. 8, 1988, pp. 1576–1587.

[5]*Project Plan for the Stanford University—NASA Laser In-Space Technology Experiment (SUNLITE)*, NASA Langley Research Center, Hampton, VA, Sept. 1990.

Recommended Reading from Progress in Astronautics and Aeronautics

Thermal-Hydraulics for Space Power, Propulsion, and Thermal Management System Design

William J. Krotiuk, editor

1990, 332 pp, illus, Hardback
ISBN 0-930403-64-9
AIAA Members $54.95
Nonmembers $75.95
Order #: V-122 (830)

The text summarizes low-gravity fluid-thermal behavior, describes past and planned experimental activities, surveys existing thermal-hydraulic computer codes, and underscores areas that require further technical understanding. Contents include: Overview of Thermal-Hydraulic Aspects of Current Space Projects; Space Station Two-Phase Thermal Management; Startup Thaw Concept for the SP-100 Space Reactor Power System; Calculational Methods and Experimental Data for Microgravity Conditions; Isothermal Gas-Liquid Flow at Reduced Gravity; Vapor Generation in Aerospace Applications; Reduced-Gravity Condensation.

Place your order today! Call 1-800/682-AIAA

AIAA

American Institute of Aeronautics and Astronautics
Publications Customer Service, 9 Jay Gould Ct., P.O. Box 753, Waldorf, MD 20604
Phone 301/645-5643, Dept. 415, FAX 301/843-0159

Sales Tax: CA residents, 8.25%; DC, 6%. For shipping and handling add $4.75 for 1-4 books (call for rates for higher quantities). Orders under $50.00 must be prepaid. Please allow 4 weeks for delivery. Prices are subject to change without notice. Returns will be accepted within 15 days.